Synthesis, Characterization, and ab Initio Theoretical Study of a Molecularly Imprinted Polymer Selective for Biosensor Materials

Rebecca Jacob,* Margaret Tate, Yididya Banti, Colin Rix, and David E. Mainwaring

School of Applied Sciences, Applied Chemistry, RMIT University, Melbourne 3001, Australia

Received: June 7, 2007; In Final Form: September 22, 2007

Despite the complex phenomena involved in encoding template molecule information within stable synthetic polymers to yield selective and efficient molecular recognition processes, molecularly imprinted polymers (MIP) are increasingly finding broad areas of application. Molecular interactions, both during the polymerization of the functional monomers in the presence of the template and during the processes of specific recognition after template removal, are key determinants of an effective MIP. Covalent and noncovalent template imprinting have been employed to achieve specific recognition sites. In the present study, a molecularly imprinted biocompatible polymer, having a high capacity and affinity for the dye template, nickel(II) phthalocyanine tetrasulfonic acid, has been prepared. UV−visible spectroscopy, FTIR spectroscopy, and ICP analysis were used to investigate the aspects of the synthesis, binding capacity, and adsorption kinetics of the system. Poly(allylamine) cross-linked with epichlorohydrin has been used to represent an amino-functional receptor. Binding isotherms and capacities were correlated with the degree of template removal. Kinetic studies of binding allowed diffusion mechanisms to be evaluated for the fine particulate MIP. Ab initio molecular orbital calculations were performed using Hartree−Fock, MP2, and density functional theory methods to determine the most likely mechanisms of molecular imprinting. Suitable theoretical models have been constructed to mimic the interactions between the template molecule and the polymer. Simulation of the vibrational spectra was also undertaken to make meaningful assignments to experimentally determined spectral bands resulting from these template MIP receptor interactions.

Introduction

Molecular imprinting of polymers is a well-established technique for the general fabrication of receptors for small molecules or biomacromolecules.[1,2] In this method, an analyte (template) molecule associates with a functional monomer(s) to form a covalent or noncovalently bonded complex. Subsequent polymerization of the mixture and removal of the analyte molecule affords an "activated" cross-linked system containing cavity imprints of a specific shape and a defined orientation of functionality within the sites. The imprinted polymer will then selectively rebind the template from a mixture of structurally related species.[3−5] These systems have useful applications in chiral separations,[6] drug delivery,[7,8] and the removal of organic contaminants from agricultural samples.[9,10] Molecular imprinting technology can be described as a way of making artificial "locks" for "molecular keys", although a more realistic description is a "hand in glove", since this recognizes the suitability of sites to allow for, and accommodate, molecular motion.

In spite of their human diagnostic potential, there has been no work where structural relatives of hemin have been investigated as possible candidates for imprinting studies in sensor applications for internal bleeding. Currently, internal bleeding is detected by surgery, X-ray tests, or a complete blood count by an authorized practitioner. Using modern technology, miniaturized video cameras with transmitters built into a capsule that is swallowed by the patient can provide images that can be transmitted wirelessly from the camera to a small pack the patient wears like a belt. During its 8-h trip through the digestive tract, the battery-powered pill uses a wide-angle lens to transmit about 50 000 images capable of identifying growths, internal bleeding, and other problems. The pill eventually passes through the colon and is eliminated naturally and safely. An imprinted polymer capable of sensing hemin would provide an alternative to these currently available methods of internal bleeding detection.

Simple metal ions have been used previously as templates in imprinting polymer matrixes,[4] but to date none have investigated large nickel(II) or iron(III) metal−ligand complexes as template compounds. We chose the template molecule, nickel(II) phthalocyanine tetrasulfonic acid, because of its similarity in structure to hemin, its rigid nature, its relative inertness to redox reactions compared to its porphyrin counterparts such as heme, and the fact that it provides an excellent probe for binding studies because of its colorimetric response in UV−visible spectroscopy. Li et al.,[11,12] in their quest for the perfect lock-and-key match of mutual chemical attractions at multilayer interfaces, have carried out the sequential depositions of oppositely charged macromolecules employing polymers such as poly(diallyldimethylammonium chloride) and oligomeric viologen, and macrocycles (ring-shaped molecules such as nickel phthalocyanine tetrasulfonic acid tetrasodium salt) using the self-assembly technique leading to the layer-by-layer growth of film structures. The success of thin-film formation was gauged using small-angle X-ray reflectometry, while spectroscopic techniques such as UV−visible and Fourier transform infrared (FTIR) were used to characterize the self-assembled structures and monitor the layer-by-layer growth.

* Corresponding author. Present address: School of Chemistry, Monash University (Clayton campus), Wellington Road, Clayton, Victoria 3800, Australia. Telephone: (61 3) 9905 3878 and +61 434 515 432. Fax: (+61 3) 9905 4597. E-mail: Rebecca.Jacob@sci.monash.edu.au or Rebecca.Jacob@rmit.edu.au.

10.1021/jp074405i CCC: $40.75
Published on Web 12/21/2007

The functional polymer system utilized in the present study, poly(allylamine) hydrochloride (PAA.HCl), is a biocompatible, water-soluble polymer that has been previously molecularly imprinted to produce hydrogels capable of adsorbing glucose and cholic acid for potential human health applications where adsorption of these compounds within the digestive tract would lead to treatments for diabetes and high cholesterol levels.[1−3] Such hydrogels are examples of cross-linked gels produced from a post-cross-linking reaction between excess functional monomers on opposite long chains or via other monomers introduced into the network.[7] In these systems, binding interactions between the template molecules and macromolecular chains are enhanced, and then cross-linking is induced to establish relatively rigid three-dimensional networks. Cross-linking was achieved with the use of epichlorohydrin after the template had assembled within the polymer network. In the remainder of this article, the term "prepolymer" will refer to the poly(allylamine) system before cross-linker has been added.

Computational approaches, such as molecular modeling, have been used in the molecularly imprinted polymer area to guide synthesis and performance by the design of virtual libraries that screen the best possible functional monomers for the preparation of a molecularly imprinted polymer (MIP) for a specific template (targets).[13−17] Ab initio calculations[18] are quantum chemical calculations that use exact equations involving the whole electronic population of the molecule and have also been used recently in the MIP area.[19,20] Published studies have given binding energies between functional monomers and target (template) molecules and the hydrogen bonding ability of several templates with a functional monomer. The energies and hydrogen-bonding abilities have then been used to further discuss the observed capacity factors and polyclonality within the MIP systems.

In this work, substrate binding and capacity investigations were undertaken using UV−visible and FTIR spectroscopic analyses as methods for monitoring the specificity and selectivity of binding of the template at the functionalized cavities. Additionally, molecular modeling and theoretically predicted FTIR spectra at various stages of the MIP synthesis have complemented our understanding of the nature of molecular recognition and associative bonding in this polymer system.

Experimental Section

Materials. PAA.HCl $[-CH_2-CH(CH_2-NH_3^+Cl^-)-]_n$ (average M_w ca.70 000), hemin chloride, and nickel(II) phthalocyanine tetrasulfonic acid tetrasodium salt were obtained from Sigma-Aldrich. Epichlorohydrin and all other organic solvents were of LR grade and purchased from BDH. Ammonia used in the wash step was a 2 M solution. All experiments were performed in aqueous solutions, freshly prepared in deionized milli-Q water.

FTIR Spectroscopy. Spectra were recorded on a Perkin Elmer FTIR spectrometer 2000 between 4000 and 400 cm^{-1}. A total of 16 scans were recorded for each spectrum. For measurements in transmission mode, standard KBr pellets were prepared.

UV−Visible Analysis. Spectra were recorded on a Varian UV−visible spectrometer Cary 1C between 200 and 800 nm using quartz cells having 0.5-cm or 1-cm path lengths.

Preparation of Molecularly Imprinted Polymer for Nickel(II) Phthalocyanine Tetrasulfonic Acid Tetrasodium Salt. A typical MIP hydrogel (MIP) was synthesized as follows: PAA.HCl (0.5 g; 5.5 mmol based on amine content) was dissolved in water (5 mL), and the pH of the solution was adjusted to 9 with 2 M NaOH. A solution of Ni(II) template (0.102 mmol in 8 mL of sodium hydroxide) was then added. The solution was then refluxed at 65−70 °C, with stirring, for 40 min before adding the cross-linker, epichlorohydrin (4.3 mmol). Gelation occurred within 5 min of adding the cross-linker, but the blue reaction mixture was heated and stirred for an additional 20 min, after which time the gel was cooled and the solid collected by suction filtration. The template was extracted by extensive washing with water, ammonia, sodium hydroxide, and finally dimethyl sulfoxide (DMSO). The removal of NaOH solution was confirmed by testing the pH of the effluent water washes. Removal of the template molecule was monitored by UV−visible spectroscopy of the wash liquors. The blue gel was dried under vacuum at ambient temperature to yield 0.815 g of the MIP. A control polymer (CP) was prepared in the same way except that the template molecule was omitted during the whole process and the solution was heated to 40 °C for 30 min before homogeneity of the reaction mixture was observed. The extensive washing process was not carried out for the CP, but the cross-linked polymer was ultrasonicated in water to remove residual base. Both the MIP and CP products were analyzed by FTIR.

Inductive Coupled Plasma (ICP) Analysis of Template Removal before Solvent Extraction. Standards of the imprint molecule were prepared for ICP (2, 4, 6, and 8 ppm Ni(II) template in 2% nitric acid), and a calibration plot was constructed. The collected washes (10 mL) after suction filtration of the polymerization reaction mixture were diluted with water (250 mL), and then nitric acid (2 M, 38 mL) was added to adjust the solution pH to 2. This solution was then made up to 500 mL with water and analyzed by ICP.

Rebinding Experiments. For batch adsorption, a specific amount (100 mg) of Ni(II) template MIP was stirred at room temperature for 90 min in 40 mL of pH 9 aqueous Ni(II) template test solutions having concentrations of 20, 40, 60, and 80 ppm. The amount of template adsorbed onto the Ni(II) template was estimated by UV−visible analysis of the filtered aliquots to determine the remaining template concentration in the test solution. Kinetic studies were also conducted in this way with the MIP being stirred in solutions of differing concentrations for the following contact periods: 5, 10, 15, 20, 30, 60, and 90 min. Selectivity of binding was conducted in a similar manner on both the control (nonimprinted) polymer (CP) and the nickel-complex imprinted polymer (MIP) by comparing the binding capability and affinity at 5 and 90 min using a 10 ppm hemin solution.

Extraction of Readsorbed Template. The removal efficiency of rebound template from the MIP, by washing with solvents after adsorption, was assessed by analyzing the FTIR spectrum of the MIP after several contact periods of 30 min in NaOH (2 M), HCl (2 M), and DMSO.

Results and Discussion

Synthesis of the Nickel(II) Phthalocyanine-Templated Polymer. The imprinted polymer was prepared by cross-linking commercially available poly(allylamine) hydrochloride, an amino-functional polymer (the receptor), in the presence of nickel(II) phthalocyanine tetrasulfonic acid (tetrasodium salt) as the model substrate molecule. Polymerization and gelation of the receptor polymer with the substrate molecule were performed in the presence of the cross-linking agent, epichlorohydrin (Figure 1).

A molecularly imprinted biocompatible polymer, having a high capacity and affinity for the dye template, nickel(II)

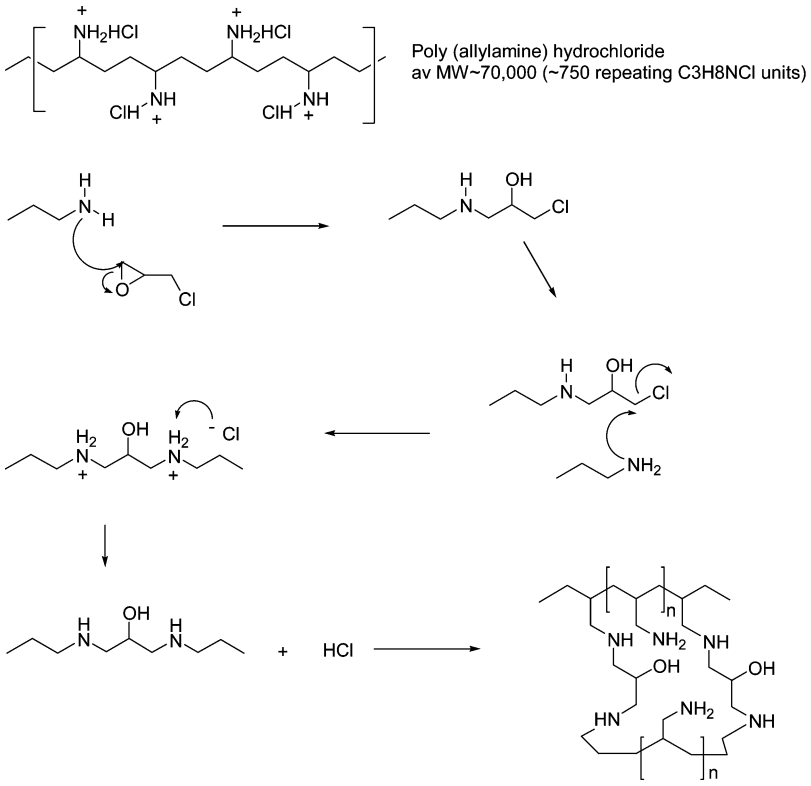

Figure 1. Reaction mechanism between epichlorohydrin and poly(allylamine).

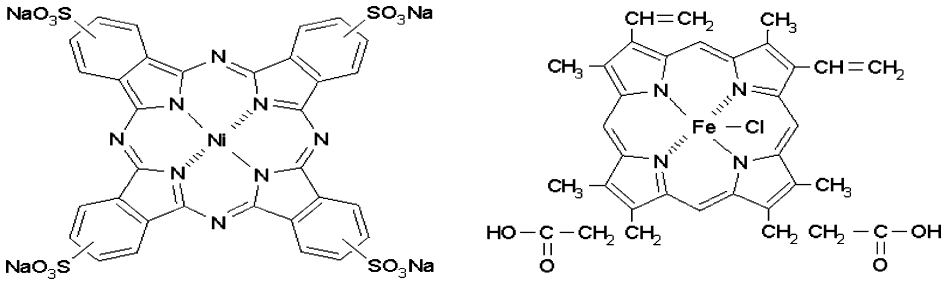

Figure 2. Chemical structures of nickel(II) phthalocyanine tetrasulfonic acid and hemin.

phthalocyanine tetrasulfonic acid, was thus prepared. The imprinting process was conducted in an alkaline solution at pH 9, which was chosen to ensure the functional polymer was partially neutralized to enable cross-linking to occur. The free NH_2 groups were thus able to bind to the Ni(II) template and also participate in cross-linking. In our quest for the development of sensitive, selective, reusable, and robust sensors for the determination of agricultural and human diagnostic applications, the Ni(II) template was selected as the model imprint compound because of its structural similarity to hemin (Figure 2), with the aim of developing an MIP-based system that could be used to detect and quantify either type of molecule. Though both hemin and the Ni(II) template are structurally related inasmuch as both have similar sizes and shapes, their functional groups are different.

Poly(allylamine) hydrochloride contains a monomeric amine group that imparts significant flexibility upon the produced MIP with respect to the number of templates for which the polymer may be imprinted. This is due to the capacity of the amine to participate in ionic interactions with anionic species as well as its propensity for hydrogen bonding. In this work, the amine is used to form an ionic association with the template's sulfonate groups. It may also interact with the nickel(II) phthalocyanine tetrasulfonic acid template through nitrogen coordination with the nickel center ($N_{polymer} \rightarrow Ni_{template}$). In addition, the epichlorohydrin cross-linking reaction produces alcohol hydroxyls (which may deprotonate in the alkaline conditions used) that could potentially participate in charge repulsion interactions. These various binding interactions can all contribute to the assembly process during the imprinting mechanism. In noncovalent assembly, the association constant between the template molecule and the functional polymer is relatively low; therefore, an excess of the functional prepolymer is required to saturate the recognition sites and the subsequent removal of the template leaves a heterogeneous population of binding sites.[10] A strong binding heterogeneity is a significant problem in this imprinting methodology, but the relative simplicity of the process makes it a goal worth pursuing.

The heating period before cross-linker addition promotes interaction of the Ni(II) template with the partially neutralized polymer chains, thereby enhancing the selectivity of the network produced. On the other hand, it has been reported that higher temperatures can be detrimental to the imprinting process, because of the influence of residual vibrational modes in monomer/polymer template interactions and also by decreasing the strength of associative interactions between the template and the monomer/polymer system.[5,6] It has been proposed that less well-defined complexes are formed at higher temperatures. The rate of polymerization is quicker at higher temperatures, and less control under such conditions may produce less homoge-

neous materials. Therefore, the existence of a finely tuned trade-off between the extent of polymerization and the stabilization of the template-functional monomer/polymer complex and optimal conditions for each combination of template and monomer/polymer requires investigation.

As reported elsewhere, epichlorohydrin was used as the cross-linker for the poly(allylamine) hydrochloride system, as it was shown to give higher specificities for the resultant imprinted polymer when compared to other linkers.[1] A large cross-linker concentration in the polymerization reaction solution (78% mol/mol of polymer chain) ensured a highly interconnected matrix was produced to entrap the template associated within the polymer matrix. The effectiveness of this was demonstrated when the imprinted gel was cooled and filtered. ICP analysis of the filtrate showed that the amount of Ni(II) template bound to the MIP accounted for 99% (0.202 mmol/g of the polymer) of the original template concentration, leaving just 1% (0.002 mmol/g) of the template molecule in the reaction mixture filtrate, suggesting that the template was effectively trapped within the wet hydrogel before solvent extraction.

Extraction of Labile Template Molecules from the MIP. Template removal is an essential step in the procedure as it is the key to providing accessible vacant recognition sites for the reuptake of the template. This was achieved by washing the imprinted, cross-linked polymer by stirring it with warm water, dilute ammonia, sodium hydroxide, and DMSO before separation via centrifugation. The water washes removed residual base and ammonia (which washed away labile template), and the DMSO swelled the saturated hydrocarbon chains and allowed the template molecules to escape, leaving imprinted cavities. The process was carried out over 66 h and was conducted on the moist cross-linked reaction product, because upon drying, the gel became rigid, which interfered with the ability of the wash solvent to penetrate the matrix to remove labile template. The lengthy extraction removed 60% (0.122 mmol/g) of the template from the MIP so the polymer still retained a light-blue color indicating that residual Ni(II) template remained trapped within the polymer gel (39%, 0.082 mmol/g).

It should be noted that no attempt to crush and sieve the MIP, or the control polymer, was made in an effort to expose more surface area to the solvent washing as it has been reported that these steps can potentially damage imprinted sites leading to a highly heterogeneous binding site distribution in the MIP.[8]

Molecular Recognition by Rebinding Experiments, MIP Capacity, Available Binding Sites, and Imprinted Polymer Selectivity. To verify the imprinting effect, samples of the imprinted polymer (MIP) and control polymer were both stirred in separate solutions of a known concentration of the Ni(II) template. Figure 3 shows the uptake of the nickel template by both the control (non-imprinted) and imprinted polymers.

The adsorption isotherm rises steeply at low concentrations of the template and thereafter reaches a saturation value at an equilibrium concentration of 40 ppm. This sharp rise follows high-affinity Langmuirian behavior. Note that the control polymers' (nonimprinted) isotherm of template adsorption onto the MIP is observed to display low-affinity, nonspecific binding and was less than 0.01% of the amount adsorbed by the MIP under comparable conditions of template concentration and temperature. The MIP reduced an initial template concentration of 40 ppm Ni(II) template (41 μmol/L) to an equilibrium concentration that was about 4% (1.77 μmol/L) of the original value. The equilibrium amount of bound template adsorbed by the MIP was calculated to be 15.6 μmol/g, hence the maximum

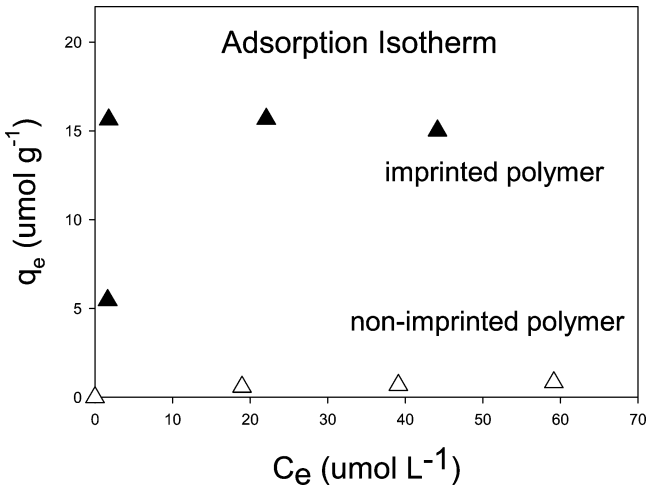

Figure 3. Adsorption isotherms (20 °C) for Ni(II) template imprinted polymer in equilibrium experiments. [Ni(II) template bound by the polymer (μmol/g) vs equilibrium concentration of Ni(II) template in solution (μmol/L)]. The experimental data were fitted to a Langmuir isotherm.

capacity for uptake of Ni(II) template from solution is 0.0157 mg of Ni(II) template/g of MIP.

The theoretical maximum capacity of the imprinted polymer, given that 60% of the incorporated template was able to be removed from the MIP matrix after extensive washing, was calculated to be 122 μmol/g, and on the basis of the amount of Ni(II) template taken up by the MIP on readsorption (16 μmol/g), the percentage of available vacant binding sites in the washed MIP was calculated to be 10.6%. This is in agreement with previous studies where it was reported that 10% of imprinted sites are able to rebind the template in imprinted polymers prepared by traditional bulk polymerization processes.[8] This proportion of imprinted sites also corresponds to the binding cavities that remain unaltered during cross-linking and after extraction.

The unavailable binding sites were calculated to be 49.4% (106 μmol Ni(II) template/g of MIP). These inaccessible cavities result from the presence of residual imprint molecules deep within the macromolecular matrix, trapped by localized cross-linking, so these binding clefts do not offer void space for analyte adsorption and are inactive.

The binding phenomenon exhibited behavior typical of a simple Langmuir adsorption model and, from Figure 4, the density of effective recognition sites on the polymer could be determined. The Langmuir isotherm, with a correlation coefficient (R^2) of 0.997, yielded an adsorption (binding) capacity of 14.9 μmol/g, a value which is in close agreement with that determined experimentally (15.6 μmol/g). The good fit of MIP adsorption to the Langmuir isotherm suggests that a unimodal heterogeneous distribution of binding sites was present in the Ni(II) template MIP.

Adsorption Kinetics. To ascertain the time required for the adsorption equilibrium to be attained, a kinetic study was carried out for the nickel template standards at four different concentrations: 10, 20, 40, and 60 ppm. Figure 5 demonstrates that equilibrium is attained after 90 min of contact at the higher template concentrations (40 and 60 ppm) studied.

For these higher concentrations, the gradient of the curve is greatest in the first 5 min, which indicates that most of the template is removed from solution by the imprinted polymer within this time. Indeed, during the first 5 min of contact between the MIP and any of these solutions, regardless of the

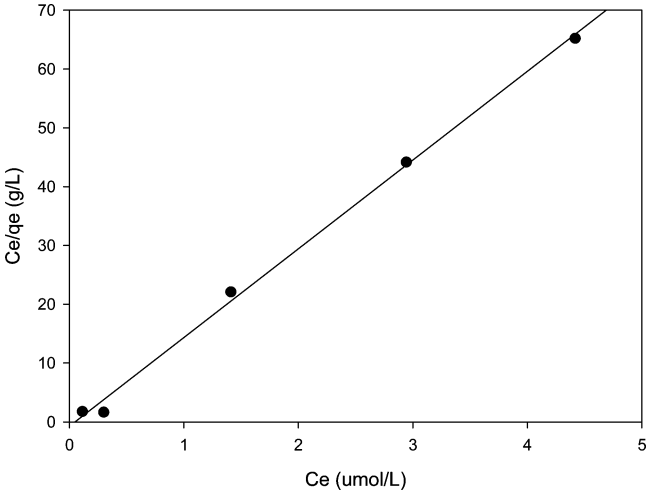

Figure 4. Langmuir isotherm (20 °C) for the Ni(II) template imprinted polymer in equilibrium experiments. [C_{equil}/q_{equil} (g/L) vs C_{equil} (μmol/L)].

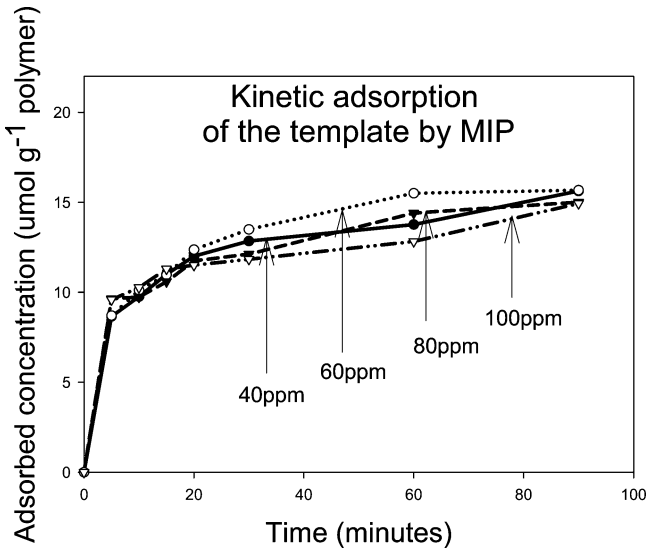

Figure 5. Kinetic adsorption of the template by MIP over 90 min [adsorbed Ni(II) template (μmol/g) vs time (min)].

concentration of template solution, more than half of the available cavities are filled, and after about 30 min, more than 80% of the sites are occupied. The rate of adsorption decreases appreciably after this time and attains a saturation value at 90 min for the more concentrated solutions and at about 30 min for solutions with concentrations of 20 ppm and below. All solutions tested start to plateau after about 60 min. This data demonstrates a high binding affinity of the imprinted polymer for the template molecule.

At the lower concentrations studied, equilibrium is achieved in less than 20 min, which indicates the MIP will adsorb lower concentrations, and attain equilibrium quicker, than when a larger concentration of template is present. In fact, after 15 min, both 40 and 60 ppm solutions released the adsorbed template back into solution until the adsorbed amount was approximately 80% of what was initially taken up in the first 5 min of MIP contact with the solution. It was interesting to note that while equilibrium was obtained for the template concentration adsorbed within similar time periods for all concentrations, the difference between the initial and equilibrium template amounts adsorbed was much less (+3% difference) for the less concentrated solutions compared to this difference for more concentrated solutions (−17%). It is suggested that this phenomenon

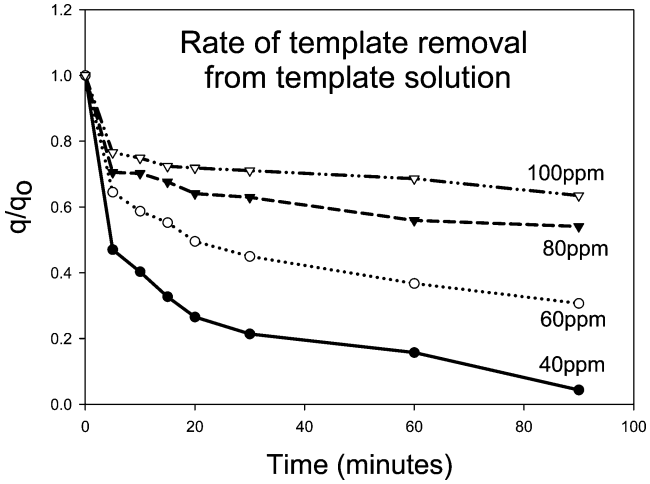

Figure 6. Rate of template removal [q/q_0 vs time (min)].

occurs because of the high affinity of the imprinted polymer for the template being limited by the amount of template in solution immediately adjacent to the MIP cavity network. The more dilute the test solution, the smaller the concentration difference of template present in the bulk solution and in this solution layer (adjacent to the MIP binding surface). Therefore, the binding of higher solution concentrations of template would still be limited by the amount of template actually present in this layer. In the case of 40 and 60 ppm solutions, the template concentration difference between the bulk solution and the solution layer is comparatively large and so, initially, the mass transfer that occurs moves a large amount of template from the bulk solution (higher concentration) into the adjacent solution layer. This is observed as a decrease in the UV−visible adsorbance of the test solution.

Removal of Template from the MIP after Adsorption. To determine whether the adsorption process is reversible, desorption tests were carried out by interacting the MIP containing the adsorbed template with appropriate solvents for a specified period and analyzing the supernatant solution for residual template content. Using these results of template uptake by the polymer, we constructed the template removal curves for each of the template solutions and show them in Figure 6. The curves indicate that, at all levels of adsorption, the template is removed rapidly during the initial 5 min of desorption. However, the degree of adsorption depends on the concentration of the initial solution used for the adsorption step, and the more concentrated solutions (which saturate the available adsorption sites) show lower release of adsorbate (template). For example, in the case of a 100 ppm adsorbate solution, only about 20% of the material is desorbed after 90 min, whereas for a similar 40 ppm solution, about 90% of material is desorbed in this time.

Template Diffusion within the Imprinted Polymer Matrix. The diffusion of template onto and into the particles of MIP was investigated, because the relatively small proportion of readsorbed template molecules indicated that not all the available binding sites were involved in this adsorption process.

Figure 7 demonstrates the linear relationship between amount of bound template and $(\text{time})^{1/2}$ and thus confirms that template diffusion follows Fick's first law, where each MIP particle is surrounded by a stagnant film of template solution, as briefly discussed in the previous section. Since the template concentration gradient between the two boundaries of the film is the driving force of adsorption, this would explain the large number of unavailable binding sites within the imprinted polymer matrix demonstrated by the low reuptake from an analyte solution.

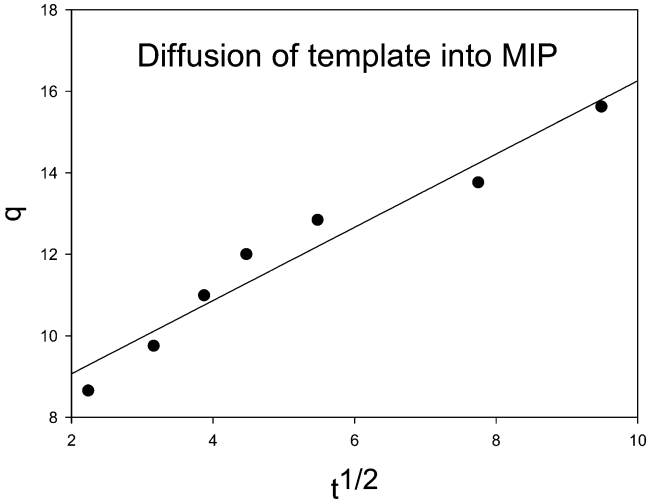

Figure 7. Characterization of the MIP template permeability.

The available binding sites in the MIP matrix that readsorbed the Ni(II) template have been proposed to correspond to those activated sites on the outer surface of each MIP particle. This would suggest that template diffusion and transport into the porous environment of the MIP or into the sites where functional groups were available (present in the binding cavities deep in the matrix) was highly unlikely. If accessibility of these sites was allowed, then uptake of Ni(II) template from solution in contact with the imprinted polymer would have been rapid and more extensive.

This film diffusion-controlled binding characteristic also affected the degree of washing of the imprinted polymer necessary to activate it toward readsorption. The experimental results indicate that 60% of the initial Ni(II) template can be removed from the MIP. This removal was from the surface and not from within the macromolecular matrix. The remaining 39% was trapped within the matrix and therefore not disturbed by surface washings.

From Figure 7, at $t = 0$, the amount of Ni(II) template bound by the MIP was $\sim 7\ \mu$mol/g of polymer, and this can be equated to the amount in the thin film before any exchange has occurred between the original solution and the particle.

MIP Selectivity Capacity and Affinity of Binding. The selectivity of the Ni(II)-templated MIP was studied by immersion of the MIP in a solution of structurally related Fe(III) compound, hemin. These experiments showed that the binding capacity of the MIP was five times higher than that of the control polymer, and the MIP had a better binding affinity for the hemin template than the control polymer. Nevertheless, the imprinted polymer binds the original Ni(II) template 3 times more effectively than the structurally related hemin complex.

The binding affinity was also determined by measuring the slopes of each adsorption curve at the initial template concentration (nickel or hemin template).

The measurements show that the MIP exhibits a binding affinity for the Ni(II) template that is 13 times higher than the affinity of the control (nonimprinted) polymer for the same template. The hemin molecule is adsorbed to a comparable amount by both the nonimprinted and the Ni(II)-templated polymer, confirming that template recognition by the imprinted polymer is governed not only by template shape and size, but also by other factors such as the nature of the functional groups on the template and the polymer.

Molecular Modeling Studies. In an attempt to gain insight into the mechanism of the imprinting process, ab initio molecular orbital calculations were performed using the Gaussian 03 program.[21] Initially, the geometry of nickel(II) phthalocyanine tetrasulfonic acid, the template molecule used in this work, was optimized at the ab initio HF/3-21G level of theory. Since the experiment was performed at pH 9.0, the complex was considered to be in the tetraanion state (charge $= -4$) with four SO_3^- groups, and the Ni(II) ion was considered to possess a low-spin d^8 configuration with no unpaired electrons (multiplicity 1). Though the central porphoryl part of the complex is symmetrical and planar, the peripheral SO_3^- groups tend to move out of the plane, thereby reducing the symmetry of the molecule. Full geometry optimization and vibrational frequency calculations were performed at the HF/3-21G level of theory to ensure the existence of a true minimum structure, with no imaginary frequencies. The geometry of hemin was also optimized at the same level of theory for comparison, with hemin being treated as a high-spin d^5 Fe(III) complex with five unpaired electrons (multiplicity 6). In this case, the central porphoryl part of the complex is also symmetrical and planar, but the peripheral substituents tend to move out of the plane, reducing the symmetry of the molecule, while the chloride ligand remains in a plane perpendicular to the porphyrin. Both molecules were of comparable size (Figure 8a−d). The most probable internuclear distances are denoted in Figure 8a,b, while the thickness of the molecule, calculated as the maximum distance the substituents protrude above and below the porphoryl plane, is denoted in Figure 8c,d. Hence, if the template is simply trapped in a cavity within the polymer network, then both hemin and nickel(II) phthalocyanine tetrasulfonate might be expected to bind with equal facility. Since there is a genuine difference observed in the selectivity of the MIP toward the two substrates, other interactions must also play a significant role.

Several types of interactions between the Ni(II) template and the polymer were considered. They included: (a) the interaction of the terminal amino groups of the polymer with the Ni(II) ion in the template, (b) the interaction of the terminal amino groups of the polymer with the porphoryl ring of the template, and (c) the interaction of the terminal amino groups of the polymer with the peripheral sulfonate groups of the template.

Previous work[22,23] has shown that although the HF/3-21G level of theory gives a good prediction of molecular structure, the level of theory has to be improved for energy predictions as well as vibrational spectra simulations. Hence, a truncated model of the Ni(II) template complex (Figure 9 in the Supporting Information) was used for calculations at higher levels of theory. This smaller model has D_{4h} symmetry, and hence density functional theory (DFT) calculations at a number of levels of theory could be readily performed. Thus, full geometry optimizations and vibration frequency calculations were performed at the HF/3-21G, B3LYP/6-31G*, and B3LYP/6-31+G* levels of theory for this truncated model.

The interaction of the Ni(II) template with the polymer was considered by studying the interaction of this truncated model of the Ni(II) template with CH_3-NH_2, the latter representing the terminal amino groups in the poly(allylamine) polymer chain. Simulations comprising different numbers of CH_3-NH_2 molecules interacting with the model Ni(II) template complex were considered. Stabilization energies for the interactions were calculated using the following relationship: stabilization energy = energy of the assembly (Ni(II) template interacting with one molecule of CH_3-NH_2) − energy of the isolated components (energy of Ni(II) template + energy of CH_3-NH_2). In this manner, the actual stabilization energy due to each interaction, such as the optimum number of terminal amino groups that

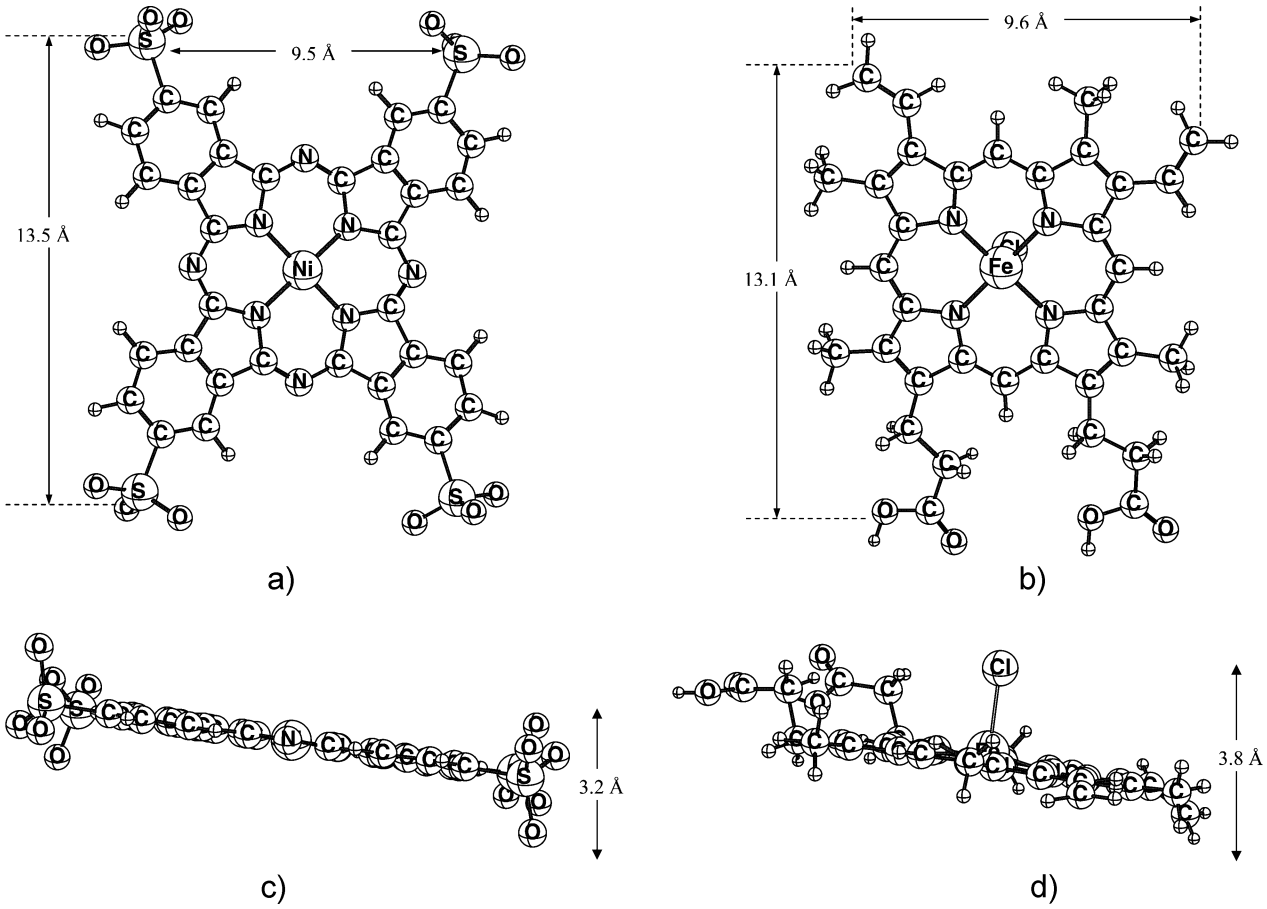

Figure 8. (a) Ab initio optimized structure of nickel(II) phthalocyanine tetrasulfonate (−4 ion). (b) Ab initio optimized structure of hemin. (c) Ab initio optimized structure of nickel(II) phthalocyanine tetrasulfonate (−4 ion), a different perspective. (d) Ab initio optimized structure of hemin, a different perspective.

TABLE 1: Stabilization Energies (SE) (in kJ mol^{-1}) at the HF/3-21G//HF/3-21G Level of Theory for the Interactions of Nickel(II) Phthalocyanine Tetrasulfonic Acid (and Its Truncated Model) with Methyl Amine (Representing the Terminal Amino Groups of the Cross-Linked Polymer) (a) for the Interaction of the Amino Group with Ni and (b) for the Interaction of the Amino Group with the N of the Porphoryl Ring

(a) model for the interaction of the amino group with Ni	SE
nickel(II) phthalocyanine tetrasulfonic acid (−4 ion) with one CH_3-NH_2	−41.9
truncated model of nickel complex with one CH_3-NH_2	−45.6
truncated model of nickel complex with two CH_3-NH_2	−73.1
(b) model for the interaction of the amino group with the N of the porphoryl ring	**SE**
truncated model of nickel complex with one CH_3-NH_2	−36.2
truncated model of nickel complex with two CH_3-NH_2	−67.9
truncated model of nickel complex with three CH_3-NH_2	−103.6
truncated model of nickel complex with four CH_3-NH_2	−137.4

stabilize the complex and the preferred orientation of the components, was calculated.

The interactions of the peripheral sulfonate groups with the polymer were calculated by considering a model benzene sulfonate anion interacting with methyl amine. The stabilization energies were calculated using the same methods as discussed above. Depending on the pH of the solution, the terminal groups could be SO_3^- or SO_3H ($pK_a < 0$) on the Ni (II) template and NH_2 or NH_3^+ ($pK_a \approx 10$) on the polymer. All these possibilities were considered.

Table 1a gives the stabilization energies of the different models representing the interaction of the terminal amino groups of the polymer with the Ni(II) ion in the template. The similarity of the interaction energy of the original nickel(II) phthalocyanine tetrasulfonate acid (−4 anion) with one CH_3-NH_2, when compared to the same interaction with the truncated model, indicates that the smaller truncated model is a very good representation of the larger template molecule. It was found that there was maximum stabilization for the interaction of two amino groups, which oriented themselves above and below the plane of the template molecule as shown in Figure 10 (in the Supporting Information). Bringing more than two amino groups in close proximity to the Ni led to destabilization. The nonbonded distance between the Ni of the template and the N of the terminal amino group of the polymer was 2.58 Å, which is quite close considering the fact that the standard bond distance for a Ni−N bond is 1.88 Å. Thus, it can be concluded that there is a weak coordinate linkage arising from partial overlap of the lone pair on the N with a vacant d-orbital on the Ni, and the directionality of this bonding interaction requires the terminal amino groups of the polymer to be orientated in the right direction on either side of the Ni(II) template.

TABLE 2: Stabilization Energies (in kJ mol^{-1}) for the Interactions of Benzene Sulfonic Acid (Representing the Peripheral Sulfonic Acid Groups of the Nickel(II) Phthalocyanine Tetrasulfonic Acid) and Methyl Amine (Representing the Terminal Amino Groups of the Cross-Linked Polymer)

	SE for the interactions of								
level of theory	$C_6H_5SO_3^-$ with two $CH_3-NH_3^+$	$C_6H_5SO_3^-$ with one CH_3-NH_2 and one $CH_3-NH_3^+$	$C_6H_5SO_3^-$ with two CH_3-NH_2	$C_6H_5SO_3H$ with two $CH_3-NH_3^+$	$C_6H_5SO_3H$ with one CH_3-NH_2 and one $CH_3-NH_3^+$	$C_6H_5SO_3^-$ with one $CH_3-NH_3^+$	$C_6H_5SO_3^-$ with one CH_3-NH_2	$C_6H_5SO_3H$ with one $CH_3-NH_3^+$	$C_6H_5SO_3H$ with one CH_3-NH_2
HF/3-21G //HF/3-21G	−761.2	−610.7	−123.7	−42.7	−196.8	−550.4	−56.4	−153.7	−34.0
B3LYP/6-31G(d) //HF/3-21G	−685.8	−550.9	−75.2	2.0	−156.4	−503.5	−41.1	−121.5	−5.8
B3LYP/6-31G(d) //B3LYP/6-31G(d)	−683.1	−551.2	−79.7	9.6	−219.8	−503.7	−41.7	−116.5	−12.6
B3LYP/6-31+G(d) //HF/3-21G	−643.4	−504.9	−50.9	10.5	−136.8	−470.2	−29.7	−111.1	2.7
B3LYP/6-31+G(d) //B3LYP/6-31+G(d)	−645.5	−512.4	−60.1	16.2	−199.2	−476.0	−32.6	−107.3	−7.8
MP2/6-31+G(d) //HF/3-21G	−614.0	−473.6	−33.7	14.0	−124.0	−445.5	−23.6	−105.4	8.2
MP2/6-31+G(d) //B3LYP/6-31+G(d)	−622.8	−487.6	−52.5	17.7	−176.3	−454.0	−29.5	−105.1	−7.7

Table 1b gives the stabilization energies of the different models representing the interaction of the terminal amino groups of the polymer with the porphoryl ring of the template. These interactions are hydrogen-bonding interactions between the H of the terminal NH_2 of the polymer and the N of the porphoryl ring of the template. From the table, it can be seen that each such interaction gives a stabilization energy of about 34 kJ mol^{-1}. The H···N distance was found to be 2.3 Å, slightly longer than strong hydrogen bonds, but much shorter than normal van der Waals interactions. The (polymer)N−H···N(on the porphoryl ring of the template) bond angle was found to be 154°, which is only a slight deviation from the normal linear N−H···N hydrogen bond angles. It was also found that the C−N bond of the polymer was at right angles to the N−C bond of the porphoryl ring of the template as indicated in Figure 11 (in the Supporting Information).

Table 2 gives the stabilization energies of the different models representing the interaction of the terminal amino groups of the polymer with the peripheral sulfonate groups of the template. Since the models considered in this case were smaller, calculations could be performed at fairly high levels of theoretical sophistication. There was maximum stabilization for the interaction of SO_3^- and NH_3^+. This is to be expected, as this interaction involves strong ionic interactions between oppositely charged groups. The notable trend was that all levels of theory gave the same order of stabilization energy and similar structures for the complexes representing the various interactions depicted in Figure 12a−c (in the Supporting Information). There was very strong hydrogen bonding between the terminal NH_3^+ of the polymer and the SO_3^- of the template. The N−H···O bond distance was as short as 1.47 Å and the corresponding N−H···O bond distance was relatively short at 1.75 Å, for the interaction between the neutral terminal NH_2 of the polymer and the SO_3^- of the template. The maximum number of amino groups that could be accommodated around each sulfonic acid group was found to be two, in spite of the presence of three oxygen atoms for each sulfonic acid group. The geometry was such that one amino group had a very strong N−H···O interaction with one of the oxygens (bond distance 1.47 Å) while the other two oxygens were involved in hydrogen bonding with two of the hydrogens of the same amino group (bond distances 1.66 and 1.84 Å, respectively).

Full geometry optimizations and vibration frequency calculations were performed at several levels of theory. Comparison of the calculated vibrational frequencies with the experimentally observed infrared spectra is an important tool in structural elucidation.[24−26] Recently, Alexander and Dines,[27] in the simulation of the vibrational spectra of ethene transition-metal complexes, especially those of Ni(II), using ab initio methods, have found that hybrid DFT functionals, specifically B3-LYP, afford the most accurate fit to the experimental data. In the present work, the vibrational frequencies calculated at the B3LYP/6-31+G* level of theory showed that strong bands due to the amino stretching frequencies of the polymer were in the 3000 cm^{-1} region, while in the strongly hydrogen-bonded amino sulfonic acid complex this band was shifted to 2800 and 2400 cm^{-1}. The experimentally observed spectra of the imprinted polymer showed peaks at 2346 and 2371 cm^{-1} and then a broad, featureless absorption extending to 2830 cm^{-1} after which a band at 2853 cm^{-1} was observed. These peaks are not present in either the template or the polymer. Hence, the presence of these peaks can only be explained by the strong hydrogen-bonding interactions of the terminal amino groups of the polymer and the sulfonate groups of the template. The calculated spectra of the template models also showed strong bands in the 600−1600 cm^{-1} region, and similar bands were observed in the actual spectra of nickel(II) phthalocyanine tetrasulfonate as well. These bands were not so prominent in the models representing the imprinted polymer.

The results of the modeling studies indicate that the optimum pH for maximum interaction is when the SO_3^- and NH_3^+ groups are present along with a small proportion of NH_2 as outlined in the following discussion. Benzene sulfonic acid has a pK_a = 0.70 ($K_a = 2 \times 10^{-1}$). CH_3NH_2 is a weak base having a pK_a =10.65 (pK_b = 3.35, $K_b = 4.38 \times 10^{-4}$). Considering the imprinting was conducted in a reaction solution with a pH of 9.0, the very high ratio of $[C_6H_5SO_3^-]/[C_6H_5SO_3H]$ (2×10^8) makes the sulfonate anion the dominant species. Similarly, at a pH of 9.0 the ratio of $[CH_3NH_3^+]/[CH_3NH_2]$ is 43.8, making the protonated quaternary ammonium species more predominant. Thus, the predominant species at a pH of 9.0 are the terminal SO_3^- groups on the template and the terminal NH_3^+ groups of the polymer along with some terminal NH_2 groups of the polymer. The stabilization energy at the B3LYP/6-31+G(d)//B3LYP/6-31+G(d) for the interaction of benzene sulfonic acid (representing the peripheral sulfonic acid groups of the nickel-(II) phthalocyanine tetrasulfonic acid) and methyl amine (representing the terminal amino groups of the cross-linked polymer) was found to be −645.5 kJ mol^{-1} for $C_6H_5SO_3^-$ interacting with two $CH_3NH_3^+$ units and −512.4 kJ mol^{-1} for

$C_6H_5SO_3^-$ interacting with one CH_3-NH_2 and one $CH_3-NH_3^+$. These large negative stabilization energy values show that there is considerable binding between the template and the polymer. Table 4 (in the Supporting Information) gives the ratios of the conjugate acid/base ions present at different pH values. Both $C_6H_5SO_3^-$ and $CH_3NH_3^+$ are the dominant species in the pH range of about 2−10.

If the solution is made more basic (pH increased above 12), the predominant species will be $C_6H_5SO_3^-$ and CH_3-NH_2. The stabilization energy at the B3LYP/6-31+G(d)//B3LYP/6-31+G(d) level of theory for the interaction of $C_6H_5SO_3^-$ with two CH_3-NH_2 is only −60.1 kJ mol^{-1}, far lower than the stabilization energy at a more acidic pH. If the solution is made very acidic (pH < 1), the predominant species become $C_6H_5SO_3H$ and $CH_3-NH_3^+$. The stabilization energy for the interaction of $C_6H_5SO_3H$ with two $CH_3-NH_3^+$ was calculated to be +16.2 kJ mol^{-1}. This positive value shows that there is virtually no binding when the solution becomes very acidic. Calculations at several different levels of theory including the MP2 level of theory confirmed the above results.

The modeling studies show that the polymer tends to form a cage around the nearly planar, rigid Ni(II) template molecule. For the preparation of the MIP described here, the cross-linking of the polymer is performed at a pH of 9.0, which allows maximum binding between the template and the polymer. The terminal amino groups become spatially oriented such that there is strong hydrogen-bonding interactions between the terminal amino groups of the polymer and the sulfonate groups of the template. The cross-linking ensures that the polymer retains its templated structure. Subsequently, when the pH is lowered, the binding interactions are reduced, permitting the removal of the template. The cross-linked polymer still retains spatially oriented end groups capable of subsequent molecular recognition at appropriate pH.

In this work, the experiments were carried out at pH 9.0, as a study of the solubility of materials at various pH conditions showed that a pH of 9.0 was optimal for the reaction, with the mildly alkaline solution ensuring the existence of a significant amount of terminal SO_3^- on the template and terminal NH_3^+ on the polymer. Further binding occurs via a weak coordinate bond interaction between the terminal amino groups of the polymer and the Ni(II) of the template, as well as hydrogen-bonding interactions between the terminal amino groups of the polymer and the N of the porphoryl ring of the template. These interactions are stronger when the terminal groups are NH_2 rather than NH_3^+, thereby justifying the choice of the higher pH value of 9. All these interactions are directional, thereby ensuring that the groups are orientated in the correct manner during cross-linking of the polymer. This procedure thus leads to the preparation of synthetic polymers that are capable of subsequent molecular recognition. Thus, while the size and shape of the template determine the size and shape of the cavity in the imprinted polymer, they appear to play a minor role in subsequent molecular recognition, since the major stabilization energy contribution arises from the molecular interactions between the polymer and the template molecule.

Conclusion

An imprinted poly(allylamine) system has been prepared using standard synthetic methods, enabling the readsorption of nickel(II) phthalocyanine tetrasulfonate (in ionized form) from mildly alkaline solution. The optimum pH for the imprinting process was found to be 9.0. The imprinted polymer was found to have a capacity of 15−16 μmol template/g of MIP. A control polymer was also synthesized, but it only adsorbed 0.01% of the template, indicating that the imprinting process had produced very selective binding sites. From this work, 40% of the template used in the cross-linking step was trapped within inaccessible sites in the polymer matrix and hence could not be removed by solvent extraction. Of the "available sites", approximately 10% were reoccupied by template molecules with the remainder inactive for template uptake. Batch readsorption experiments using the imprinted polymer gave isotherms that showed characteristic Langmuirian adsorption, while template diffusion within the polymer was observed to follow Fick's law. Kinetic investigations showed the equilibration time of the imprinted system could vary between 30 and 90 min, depending on the concentration of the test solution. The method described here provides a simple procedure for the synthesis of imprinted hydrogels with high affinities for many classes of template molecules. Theoretical calculations using ab initio methods showed that the polymer tended to form a cage around the nearly planar, rigid template molecule. The terminal amino groups were found to be spatially oriented such that there were strong interactions between the terminal amino groups of the polymer and the sulfonate groups of the template.

Acknowledgment. Ab initio calculations were carried out on an HP AlphaServer Super Computer. R.J. was supported by a Research Award under the Merit Allocation Scheme of the National Facility of the Australian Partnership for Advanced Computing, ANU, Canberra.

Supporting Information Available: Additional structures and ratios of corresponding acid/base species with pH variation. This material is available free of charge via the Internet at http://pubs.acs.org.

References and Notes

(1) Wizeman, W. J.; Kofinas, P. *Biomaterials* **2001**, *22*, 1485.
(2) Huval, C. C.; Bailey, M. J.; Braunlin, W. H.; Holmes-Farley, S. R.; Mandeville, W. H.; Petersen, J. S.; Polomoscanik, S. C.; Sacchiro, R. J.; Chen, X.; Dhal, P. K. *Macromolecules* **2001**, *34*, 1548.
(3) Wizeman, W.; Kofinas, P. *Polym. Prepr. (Am. Chem. Soc., Div. Polym. Chem.)* **2000**, *41*, 1632.
(4) *Molecular and Ionic Recognition with Imprinted Polymers;* Bartsch, R. A., Maeda, M., Eds.; ACS Symposium Series 703; American Chemical Society: Washington, DC, 1998.
(5) Byrne, M. E.; Park, K.; Peppas, N. A. *Adv. Drug Delivery Rev.* **2002**, *54*, 149.
(6) Byrne, M. E.; Park, K.; Peppas, N. A. *Adv. Drug Delivery Rev.* **2002**, *54*, Ch. 2.
(7) Piletsky, S. A.; Piletska, E. V.; Karim, K.; Freebairn, K. W.; Legge, C. H.; Turner, A. P. F. *Macromolecules* **2002**, *35*, 7499.
(8) Cheong, S. H.; McNiven, S.; Rachkov, A.; Levi, R.; Yano, K.; Karube, I. *Macromolecules* **1997**, *30*, 1317.
(9) Piletsky, S. A.; Piletskaya, E. V.; Panasyuk, T. L.; El'skaya, A. V.; Levi, R.; Karube, I.; Wulff, G. *Macromolecules* **1998**, *31*, 2137.
(10) Katz, A.; Davis, M. E. *Macromolecules* **1999**, *32*, 4113.
(11) Lütt, M.; Fitzsimmons, M. R.; Li, D. *J. Phys. Chem. B* **1998**, *102*, 400.
(12) Li, L. S.; Li, A. D. Q. *J. Phys. Chem. B* **2001**, *105*, 10022.
(13) Chianella, I.; Lotierzo, M.; Piletsky, S. A.; Tothill, I. E.; Chen, B.; Karim, K.; Turner, A. P. F. *Anal. Chem.* **2002**, *74*, 1288.
(14) Chianella, I.; Piletsky, S. A.; Tothill, I. E.; Chen, B.; Turner, A. P. F. *Biosens. Bioelectron.* **2003**, *18*, 119.
(15) Fu, Q.; Sanbe, H.; Kagawa, C.; Kunimoto, K.-K.; Haginaka, J. *Anal. Chem.* **2003**, *75*, 191.
(16) http://www.labonline.com.au/science/feature_article/item_062001.asp.
(17) http://www.synthetic-receptors2003.com/1b.02.pdf.
(18) http://www.albmolecular.com/features/tekreps/vol02/no17/.
(19) Wu, L.; Sun, B.; Li, Y.; Chang, W. *Analyst (Cambridge, U.K.)* **2003**, *128*, 944.
(20) Mukawa, T.; Goto, T.; Nariai, H.; Aoki, Y.; Imamura, A.; Takeuchi, T. *J. Pharm. Biomed. Anal.* **2003**, *30*, 1943.

(21) Frisch, M. J.; Trucks, G. W.; Schlegel, H. B.; Scuseria, G. E.; Robb, M. A.; Cheeseman, J. R.; Montgomery, J. A., Jr.; Vreven, T.; Kudin, K. N.; Burant, J. C.; Millam, J. M.; Iyengar, S. S.; Tomasi, J.; Barone, V.; Mennucci, B.; Cossi, M.; Scalmani, G.; Rega, N.; Petersson, G. A.; Nakatsuji, H.; Hada, M.; Ehara, M.; Toyota, K.; Fukuda, R.; Hasegawa, J.; Ishida, M.; Nakajima, T.; Honda, Y.; Kitao, O.; Nakai, H.; Klene, M.; Li, X.; Knox, J. E.; Hratchian, H. P.; Cross, J. B.; Adamo, C.; Jaramillo, J.; Gomperts, R.; Stratmann, R. E.; Yazyev, O.; Austin, A. J.; Cammi, R.; Pomelli, C.; Ochterski, J. W.; Ayala, P. Y.; Morokuma, K.; Voth, G. A.; Salvador, P.; Dannenberg, J. J.; Zakrzewski, V. G.; Dapprich, S.; Daniels, A. D.; Strain, M. C.; Farkas, O.; Malick, D. K.; Rabuck, A. D.; Raghavachari, K.; Foresman, J. B.; Ortiz, J. V.; Cui, Q.; Baboul, A. G.; Clifford, S.; Cioslowski, J.; Stefanov, B. B.; Liu, G.; Liashenko, A.; Piskorz, P.; Komaromi, I.; Martin, R. L.; Fox, D. J.; Keith, T.; Al-Laham, M. A.; Peng, C. Y.; Nanayakkara, A.; Challacombe, M.; Gill, P. M. W.; Johnson, B.; Chen, W.; Wong, M. W.; Gonzalez, C.; Pople, J. A. *Gaussian 03;* Gaussian, Inc.: Pittsburgh, PA, 2003.

(22) Henry, D. J.; Parkinson, C. J.; Mayer, P. M.; Radom, L. *J. Phys. Chem. A* **2001**, *105*, 6750.

(23) Henry, D. J.; Parkinson, C. J.; Radom, L. *J. Phys. Chem. A* **2002**, *106*, 7927.

(24) Jacob, R.; Fischer, G. *J. Mol. Struct.* **2002**, *613*, 175.

(25) Jacob, R.; Fischer, G. *J. Phys. Chem. A* **2003**, *107*, 6136.

(26) Fischer, G.; Jacob, R.; Cao, X. *Chem. Phys.* **2001**, *263*, 243.

(27) Alexander, B. D.; Dines, T. J. *J. Phys. Chem. A* **2004**, *108*, 146.